

Neighborhood, topography, and wind direction effects on wind pressure distribution on the low-rise building roof

VITOR G. O. CAMILO, MARCO D. DE CAMPOS

Institute of Exact and Earth Sciences
Federal University of Mato Grosso,
Av. Valdon Varjão, 6390, Barra do Garças, 78605-091, Mato Grosso
BRAZIL

Abstract: Low-rise buildings are the majority of the houses that are constructed all over the world. Experiments of the wind loads acting on these buildings provide vital information to design secure structures and adverse weather conditions resistants, considering the basic parameters as roof slopes and the wind direction. This study estimated the distribution of wind pressures around the contour of buildings with gable roofs, considering diverse neighborhood conditions, namely the number and geometric configuration of buildings on the ground, in conjunction with the different angles of wind incidence and topography. The simulations took place with *Ansys Workbench* software, and the *RNG K-Epsilon* turbulence model and tetrahedral mesh were employed. The application validation of the CFD technique occurred in the double-sloped pitched roof structure. The results showed good concordance with the literature. The pressure coefficients were analyzed, as well, in the flow visualization, highlighting the attachment points and the recirculation zones.

Key-Words: Wind action, low-rise buildings, neighborhood, wind incidence, topography, pressure coefficients.

Received: November 26, 2021. Revised: October 29, 2022. Accepted: November 25, 2022. Published: December 31, 2022.

1 Introduction

The most common building type used in the residential, commercial, and industrial sectors is, arguably, low-rise buildings [1]. Nonetheless, this construction typically receives low priority and limited field observation/inspection of wind loading. Consequently, they suffer the heaviest damage from high winds, entailing massive economic losses for countries [2]. The critical areas of good design and construction for wind resistance concentrate in the walls, roofs, and our connections. In particular, the roof structure provides crucial lateral support to load-bearing and non-load-bearing walls. Once the roof structure is partially or fully lost and the roof diaphragm committed, then with the stand wind pressure, there is a considerable reduction in the ability of the walls [2]. Large fluctuating wind loads originating from turbulent background winds pronounced flow separation at sharp edges of buildings (e.g., eaves and building corners), and intermittent flow separation and reattachment on building surfaces are the principal causes of wind damage to low-rise buildings [3]. Low-rise buildings are seldom tested for wind actions, while tall buildings are often so [1]. In this work, the pressure coefficients were determined for the

methodology validation, considering a single structure with double slopes, according to Fouad *et al.* [4]. On remaining applications also calculated the pressure coefficients for two and three buildings with gabled roofs. The basic parameters considered in the analysis include neighborhood conditions and wind direction.

In this work, the distribution of wind pressures with numerical tests around the contour of buildings with gable roofs, considering diverse neighborhood conditions such as the number and geometric configuration of buildings on the ground, in conjunction with the different angles of wind incidence and topography (Fig. 1 a-e).

2 Methodology

For the geometry modeling, was used *Autodesk AutoCAD* software was used. For the CFD technique validation, according to Fouad *et al.* [4], the models were placed inside the domain of 9 H width, 9H height, and 21H length (Fig. 1f). Here, H = 6 m is the maximum height of the building, in agreement with Fouad *et al.* [4]. For the other applications, considering diverse neighborhood conditions, namely as the number and geometric configuration of buildings on the ground, in

conjunction with the different angles of wind incidence, was adopted as the control volume, according to Franke *et al.* [5]. The boundaries are 5H from the inlet and both sidewalls, 6H from the model base, and 15H behind the building to allow flow development (Fig. 1g). Here, $H=3.72$ m is the maximum height of the building and boundary conditions. Table 1 shows the nondimensional parameters. The *Ansys Fluid Flow* software, and the *RNG K-Epsilon* turbulence model, were adopted for simulations.

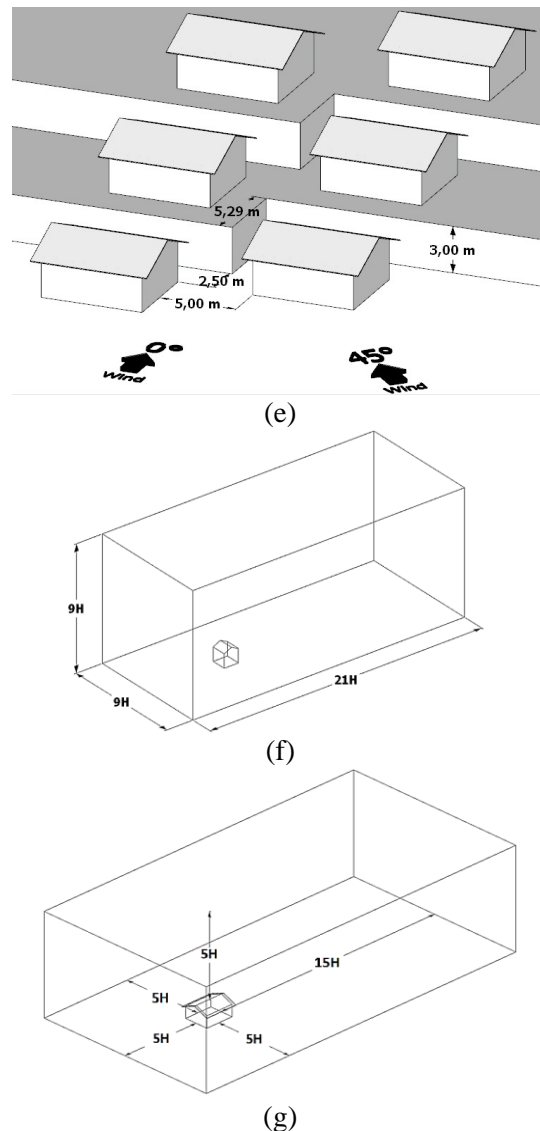
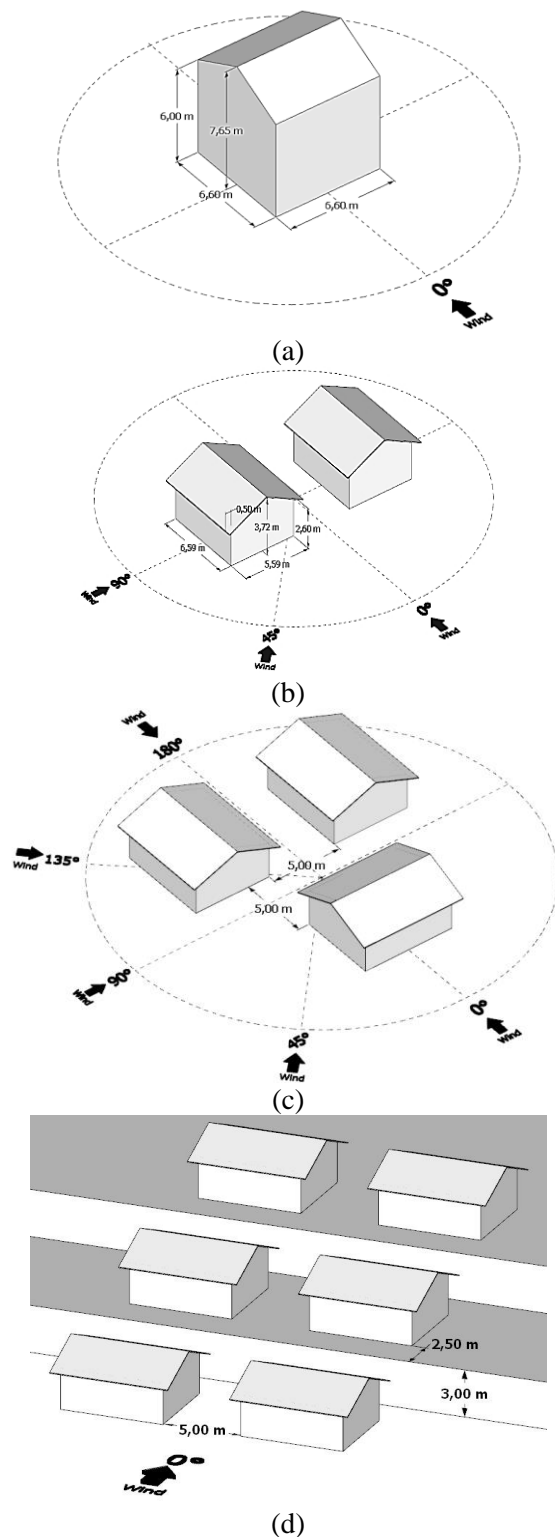


Fig. 1 (a-e) Geometry and different angles of incidence of the wind, and (f), (g) the control volume.

Table 1. Boundary conditions and nondimensional parameters.

Condition	Parameters
Method of mesh	Tetrahedron
Reference pressure	101325 [Pa]
Air temperature	25 [°C]
Specific mass	1.185 kg/m ³
Inlet	35 [m/s]
Relative pressure of outlet	0 [Pa]
Roughness	0.01 [m]
Turbulence model	<i>RNG K-Epsilon</i>

3 Numerical applications

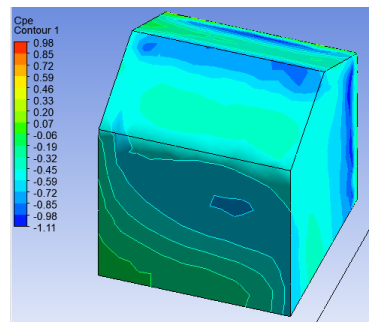
Application 1 (single structure with double slopes): This is the usual sloping roof that slopes in two directions, and the two inclinations meet at the ridge. The gable roof is permissible on any structure. The short gable roof building has a length

of 6.6 m, a width of 6.6 m, a gable height of 6 m, and a roof slope equal to 26.6° [4]. The mesh formed by tetrahedrons resulted in 2331763 elements and 489871 nodes. Here, 1.225 kg/m^3 for air density and a wind speed of 44.76 m/s incidents at 0° were adopted orthogonally to the side face of the building.

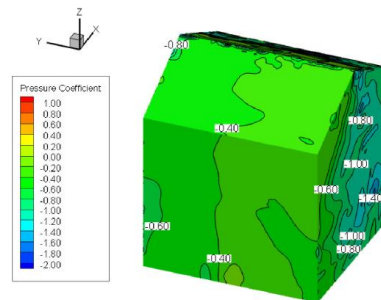
In all applications, the local pressure coefficients, defined by $C_{pe} = \Delta p / q$, where C_{pe} is the external pressure coefficient, Δp is the difference in the external pressure coefficient, and q is the dynamic pressure, were calculated.

Fig. 2 shows an agreement between the isobaric lines [4] and those generated by *Ansys* in this work. The pressure distribution values on the facades and roof are the same, with a slight change in distribution. The windward face of the building presented external pressure coefficients ranging from 0.20 to 0.98 (Fig. 1a), in line with Fouad *et al.* [4], whose values ranged from 0.00 to 1.00 (Fig. 2b). The values range between -0.85 and 0.07 (Fig. 2c) diverge from Fouad *et al.* [4] on the leeward side. The coverage showed the highest negative values in the windward region, with a minimum pressure coefficient of -1.11, agreeing with -1.20 in Fouad *et al.* [4]. The downstream section showed values similar to those in the literature of -0.19 (Fig. 2c-d).

Then, to determine significant differences between the present work results and the literature, the *T-test* was used, considering a null hypothesis that the means are not different. Thus, considering a one-tailed distribution, $p\text{-value} = 0.43$ was obtained for a critical $t = 1.81$. As $0.43 < 1.81$, it was possible to conclude that the difference between the mean values of C_{pe} is insignificant.



(c) Present work



(d) Fouad *et al.* [4]

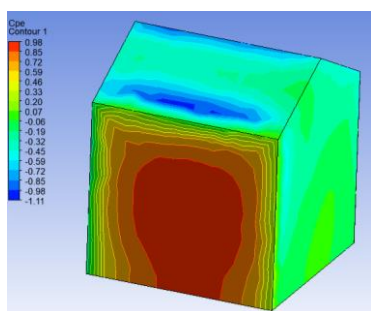
Fig. 2. Flow pressure distribution of the (a), (b) windward, and (c), (d) leeward facades.

The following applications simulated the flow with different wind incidence angles. It was considered a wind speed of 35 m/s acting on two and three buildings opening with double slopes. Next, will be investigated two configurations for different wind incidence angles (0° , 45° , and 90°) (Fig. 1b-c).

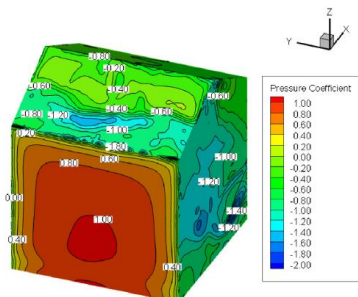
Application 2 (two buildings side-by-side with double slopes)

Case 1 (incident wind at 0°): The color hue represents the pressures on the building surface, corresponding to the external pressure coefficients. Cool colors represent suction regions, while warm colors represent overpressure regions (Fig. 3a). Fig. 3 shows the streamlines. Vortex shedding in the structure was evident with the wind at 0° (Fig. 3b). This phenomenon consists, basically, of the retardation of air particles due to friction with the surface, where small masses of dammed air detach and flow away from the course and, as the air moves, there is a change in pressure at the surface, according to Leet *et al.* [6].

Case 2 (incident wind at 45°): When the wind blows obliquely onto the corner of a roof, a flow pattern appears with the conical vortices formation similar to those found at the ends of airplane wings, according to Holmes [7]. They constitute a discharge of the existing vorticity in the aerodynamic field around the construction. They are responsible for any accidents, with partial or total removal of the roof of buildings due to the intense suction caused, according to Blessmann [8].



(a) Present work



(b) Fouad *et al.* [4]

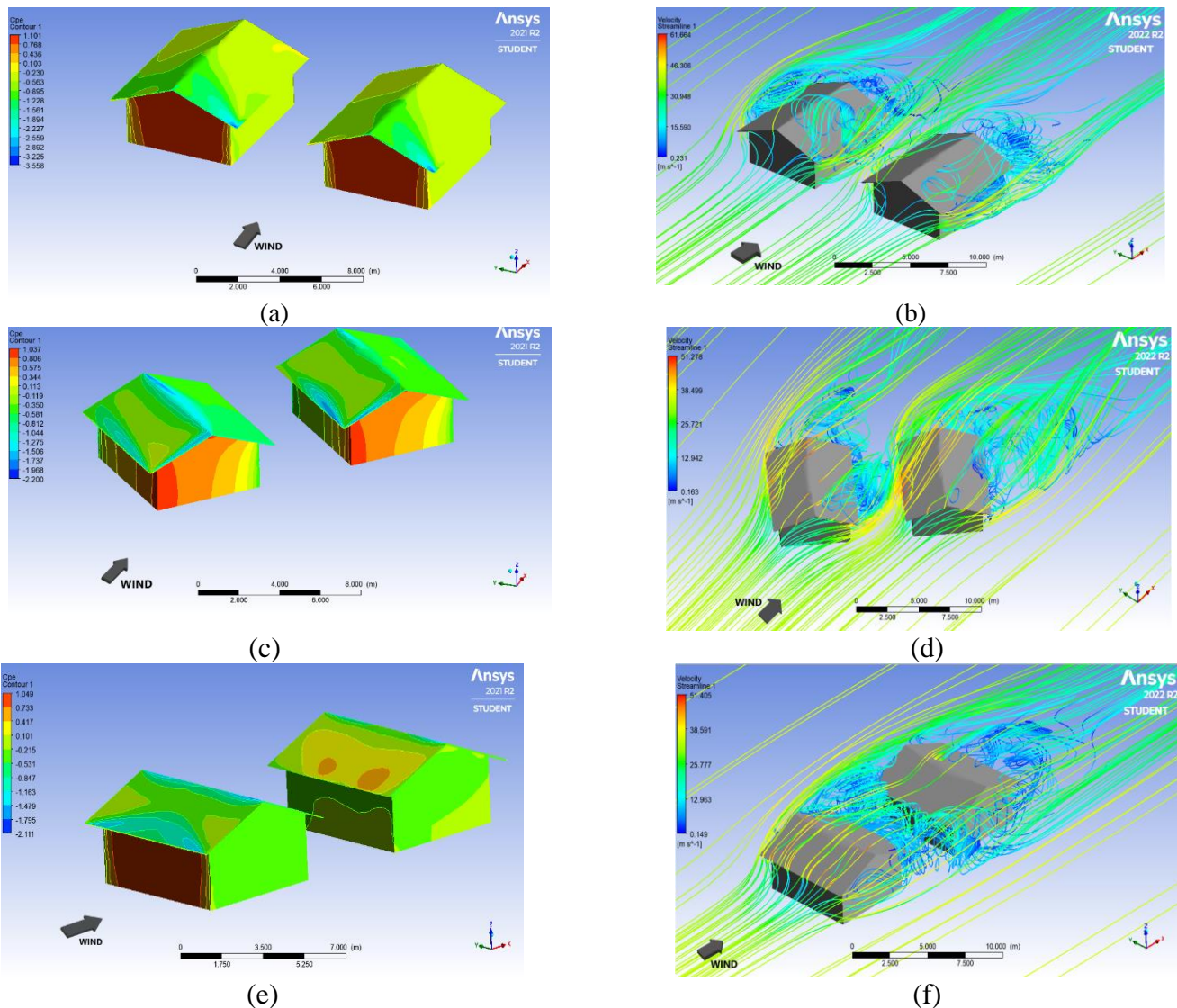


Fig. 3. C_{pe} and streamlines for the wind incident at (a), (b) 0° , (c), (d) 45° ; (e), (f) 90° in the buildings.

The conical-shaped vortex extends along both roof edges. This area will be vulnerable to highly fluctuating and extreme forces. In this case, the pressures are among the highest that occur in low-slope roofs, with square or rectangular plants, although, generally, the affected areas are small. According to Fig. 3c, there was a reduction in $C_{pe_{max}}$, which is more intense in the corners of buildings where the wind hits.

The largest suction zones occur at the corners of the eaves of the buildings. They appear paired originated by the top vortex's conical-helical shape from the corner of the building to the windward side (Fig. 3d). The suction values in this region reached, in the module, values between 2.0 and 3.0, in agreement with Blessmann [8].

Case 3 (incident wind at 90°): The largest overpressure zones are formed on the windward face of the building when the wind is perpendicular to one of the facades. Between them, the external

pressure coefficients are negative (Fig. 3e). The base vortices between buildings were the cause of these suctions (Fig. 3f). These vortices, in turn, originate near the ground with an approximately horizontal axis. Then, they develop helically from the facade center until the two ends, escaping through the sides with increased speed [8].

Small changes in overpressures on the windward façade are due to base vortices. Close to the side facades, they caused increased local velocities (Fig. 3e) and, as a result, high suctions with pressure coefficients reached, in a module, between 1.5 and 2.0 (Fig. 3f), in agreement with the literature [8].

Application 3 (three buildings with double slopes): In the same conditions as the previous application, three buildings abreast with double slopes, were considered wind incidence angles 0° , 45° , 90° , 135° and 180° (Fig. 1c).

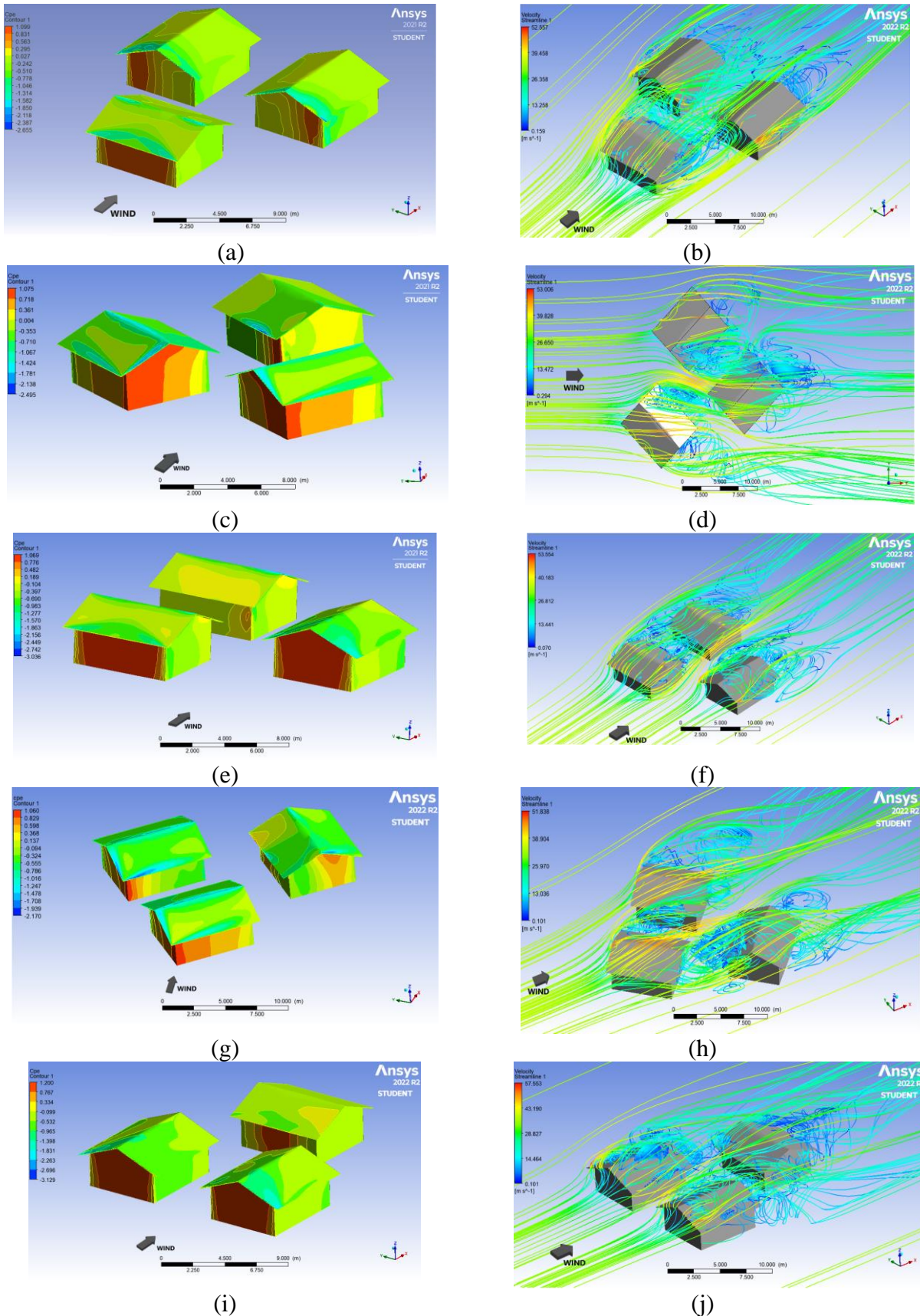


Fig. 4. C_{pe} and streamlines for the wind incident at (a-b) 0° , (c-d) 45° ; (e-f) 90° , (g-h) 135° and (i-j) 180° in the buildings.

Case 1 (incident wind at 0°): With the wind at 0° , the building added to the windward side presented high overpressure on the wind's face. The increase in wind speed passing through the building

originated from a suction at the corners of the roof, represented by cold colors in Fig. 4 a-b.

For the buildings arranged side by side, there was a decrease in the maximum values of the

contours of the maximum pressure coefficients. This fact resulted in smaller overpressure zones. In these buildings, the largest suction zones were also detected, provoked by the leeward base vortices of the first building in addition to the wake interference flow regime. There, an attempt to reconstitute the atmospheric boundary layer occurs, which did not happen due to the proximity of the constructions, making the flow turbulent enough for an unbalanced formulation of vortices incident on the leeward structure (Fig 4b).

Case 2 (incident wind at 45°): Here, an abundance of vortices was formed and, consequently, areas with higher pressure coefficients (Fig 4c-d) due to the incidence of wind in the corners of the buildings. These corners of the buildings on the windward side presented the highest zones of overpressure ($Cpe_{max}=1.075$). The top vortices caused intense suction in the corners of the eaves of the buildings. The suction values in this region reached, in the module, $Cpe_{min} = 2.495$, in agreement with [8]. These vortices can damage the building's structure, both for the generating structure and the receiving building [9].

Case 3 (incident wind at 90°): The windward faces had the highest overpressure zones, with the wind perpendicular to the buildings. The external pressure coefficients are negative on the faces between the buildings (Fig. 4f). As a result of wind funneling between very close edits and accelerating the airflow, the Venturi effect generated these suction. When the wind reaches the first building, the base and top vortices form on the roof. Consequently, the flow acceleration originates in an intense suction region in the inner part of the ridge with values, in module, of 3.036. (Fig. 5).

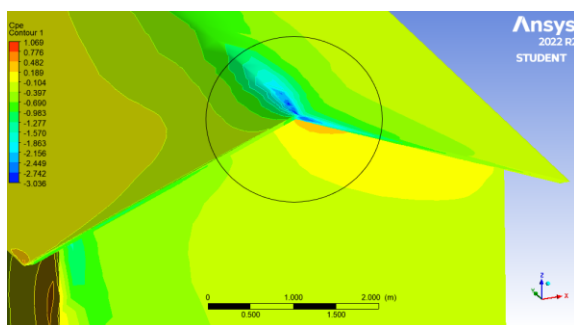


Fig. 5. Intense suction region on the inside of the ridge (detail)

Case 4 (incident wind at 135°): In this situation, similar to the wind blowing at 45°, the flow with the most intense overpressure zones occurred at the corners, mainly in the building where the wind hit first, showing the maximum coefficient contours of positive pressure there. In addition, there was the formation of top vortices with conical shapes, which

created intense suction zones on the eaves of the buildings (Fig 4g-h).

The third building to leeward received the direct incidence of the wind, and it was possible to notice the random formation of positive and negative contours. The other part suffered from the impact of vortices released from other edifications.

Case 5 (incident wind at 180°): In this case, the front facades of the two buildings on the windward side showed large overpressure areas, as the wind blows orthogonally to these faces, having greater intensity (Fig 4i). The channeling of the wind between the two buildings, called the Venturi effect, caused the flow to gain speed, generating suction on the internal side faces. In addition, this flow channeling originated zones of intense overpressure in the leeward building, in which the pressure coefficient reached 1.2.

In Fig. 4j, the streamlines show the shedding of vortices that occurs when the wind passes through buildings, which makes the flow disordered and creates zones of intense suction on the roof of buildings. Fig. 6 details the corner of the eaves of the edification positioned on the left, where the most intense suction zone was found (3.129 in module). The top vortices in the incidence of the wind at the edge of the eaves caused this suction [8].

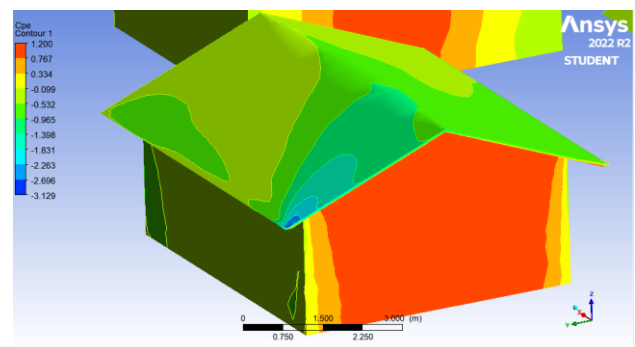


Fig. 6. Intense suction region on the corner of the eaves (detail).

Application 4 (influence of topography): The wind speed value grows with height; furthermore, topographical features such as escarpments in flat open terrain have a quite strong impact on wind speed profiles.

Case 1 (slopes and aligned buildings): In this case, the wind blowing perpendicularly on the windward buildings caused the largest overpressure zones. The leeward structure, favored by the geometric configuration on the terrain, generated the minor zones of positive pressure due to the shielding effect (Fig. 7a). The incidence of wind on a hill or slope causes the increase of the velocity of flow due to the Venturi effect. This effect will be maximum for the wind blowing perpendicular to the ridge line and a slope or hill with large width [10]. Fig. 7b

shows this phenomenon with the streamlines, and it is possible to observe the gain in wind velocity along the runoff and the increase in height, generating intense suctions on the ridges of the roofs of the buildings arranged on the second slope.

Case 2 (slopes with lateral height difference): Considering, now, buildings on the slopes with lateral height differences, the windward building on the left side, on the first slope, had minor zones of overpressure compared to the building on the right. The shielding effect of the slope attenuated the wind effects, while the building on the right side at ground level received the direct incidence of the wind (Fig. 7c).

Also, in this case, the Venturi effect generated an increase in the runoff velocity (Fig. 7d), causing the highest overpressure regions in the buildings on the second and third slopes on the left side, with intense suction on the roof of the building on the summit (Fig. 7c).

On the right side of the flow, the direct incidence of the wind on the first building generated intense vortex formation (Fig. 7d). As the turbulence generated energy dissipation, the wind impacted the buildings on the leeward side with less intensity, thus causing milder pressure coefficients under these conditions.

Case 3 (slopes with different depths): Here, with other depths in the slopes, the largest zones of overpressure were found in the lateral faces of the windward buildings, being the most expressive in the left edification, and there was a greater region of turbulence and vortex shedding.

For edits to the right, we have the smaller overpressure zones resulting from lower incident wind speed (Fig. 7e-f).

Fig. 7e shows the intense suction on the roofs of the buildings at the top of the slope.

This suction, generated by the topographical unevenness, is a consequence of the increase in runoff velocity.

Case 4 (slopes with different depths and wind at 45°): Finally, with the slopes of different depths and the incident wind at 45°, a more complex situation originated due to the incidence of the wind on the edges of the slope, and the buildings.

Fig. 7 g-h shows a formation of the top vortices causing intense suctions on the edges of the eaves and ridges of the roofs and, in a certain way, increasing the chance of roof collapse and total or partial destruction of the roofing (Fig. 7g-h).

The distribution of the pressure coefficients showed that the shielding effect protected the building on the left side of the slope. On the other hand, the building to its right presented positive contours on its front façade and intense suction on

the roof due to the direct incidence of the wind with higher velocity (Fig. 7h).

4 Conclusions

This paper presented the distribution of wind pressures with numerical tests around the contour of buildings with gable roofs, considering diverse neighborhood conditions such as the number and geometric configuration of buildings on the ground, in conjunction with the different angles of wind incidence and topography obtained from *Ansys Workbench* software.

For validation methodology, a single structure with double slopes, according to [4], was considered. In the leeward face, the comparison of the distribution of isobaric lines showed a difference.

The values coincided in the windward facade and the roof. Three orthogonal incidences for low-rise building design purposes have presented the results for external pressure coefficients.

With the wind at 0° and the addition of the third building, there was a decrease in the contours of the maximum coefficients in the leeward structure, indicating smaller overpressure zones compared to the two-building model. However, there were the highest suction zones noticed in these conditions. This effect is to the leeward vortices in the first building and the flow interference in the wake.

Now, when the wind is at 45° and the third building, there was an increase in areas with higher pressure coefficients compared with the two-building model. In this case, the most intense suction zones occurred in the corners of the eaves of the buildings. Furthermore, with the wind at 90° in two buildings, the largest overpressure zones were formed on the windward face of the building when the wind was perpendicular to one of the facades. High suction also occurred, caused by increased local velocities. With the presence of the third building, the suction on the faces between the buildings intensified. Due to the increase in wind speed at the leeward ridge of the building, there was intense suction.

With the incident wind at 135°, similar to the wind blowing at 45°, intense overpressure zones occurred at the corners, mainly in the building where the wind hit first. In addition, there was the formation of top vortices with conical shapes. The third building to leeward received the direct incidence of the wind, and it was possible to notice the random development of positive and negative contours. The other part suffered from the impact of vortices released from other edifications.

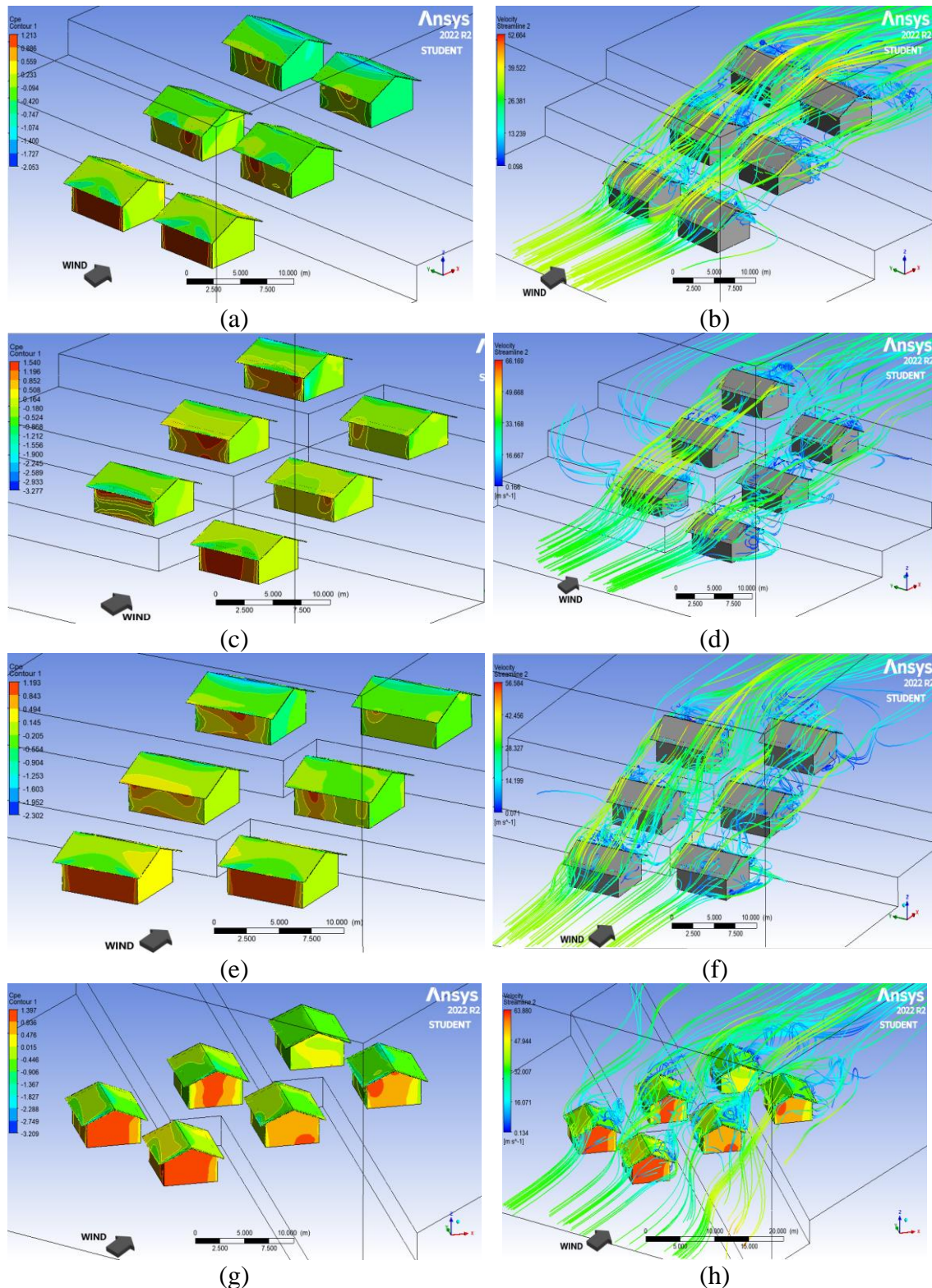


Fig. 7. *Cpe* and streamlines for (a-b) slopes and aligned buildings, (c-d) slopes with lateral height difference; (e-f) slopes with different depths, and (g-h) slopes with different depths and wind at 45°.

Finally, to incident wind at 180°, the front facades of the two buildings on the windward side showed large overpressure areas. The Venturi effect caused the flow to gain speed, generating suction on the internal side faces and originated zones of intense

overpressure in the leeward building, where the pressure coefficient reached 1.2.

Besides, the topography influenced slopes and aligned buildings. In this case, the wind blowing

perpendicularly on the windward buildings caused the largest overpressure zones.

On another side, the minor positive pressure zones occurred in the leeward structure. Now, for slopes with a lateral height difference, the shielding effect of the incline attenuated the wind effects. On the right side of the flow, the direct incidence of the wind on the first building generated intense vortex formation.

Already, in the slopes with different depths, the largest overpressure zones occurred in the lateral faces of the windward buildings.

In addition, there was an intense suction on the roofs of the buildings at the top of the slope. Finally, for slopes with different depths and wind at 45°, a formation of the top vortices causes intense suction on the edges of the eaves and ridges of the roofs and, in a certain way, increases the chance of roof collapse and total or partial destruction of the roofing.

Concluding, these results can motivate the elaboration of a roadmap to reduce accidents in buildings due to wind. Furthermore, this material would fill a gap for scholars in the area and could decrease low-rise roof accidents.

References:

- [1] D. P. P. Meddage, C. S. Lewangamage and A. U. Weerasuriya, On the deviation of mean pressure coefficients in wind loading standards for a low-rise, gable-roofed building with boundary walls, *Structures*, Vol. 36, 2022, pp. 50-64.
- [2] M. J. Crosbie, *Buildings at risk: wind design basics for practicing architects*. Washington: American Institute of Architects, 1998.
- [3] T. Stathopoulos, Wind loads on low-rise buildings: a review of the state of the art, *Engineering Structures*, Vol. 6, No. 2, 1984, pp. 119–135.
- [4] N. S. Fouad, G. H. Mahmoud and N. E. Nasr, Comparative study of international codes wind loads and CFD results for low rise buildings, *Alexandria Engineering Journal*, Vol. 57, 2018, pp. 3623–3639.
- [5] J. Franke, A. Hellsten, H. Schlünzen and B. Carissimo, *Best practice guide for the CFD simulation of flows in the urban environment, COST Action 732: Quality assurance and improvement of microscale meteorological models*. Hamburg: COST Office, 2007.
- [6] K. M. Leet, C. M. Uang, J. T. Lanning and A. M. Gilbert, *Fundamentals of Structural Analysis*. New York: McGraw-Hill, 2018.
- [7] J. D. Holmes, *Wind Loading of Structures*. London: Spon Press, 2001.
- [8] J. Blessmann, *Aerodinâmica das construções*, Porto Alegre: UFRGS, 2011 (in Portuguese).
- [9] J. Blessmann, *Introdução ao estudo das ações dinâmicas do vento*, Porto Alegre: UFRGS, 2005 (in Portuguese).
- [10] J. Blessmann, *O vento na Engenharia Estrutural*, Porto Alegre: UFRGS, 2013 (in Portuguese).

Contribution of individual authors to the creation of a scientific article

Vitor Camilo was responsible for the methodology, carrying out the simulation, and writing the results. Marco Campos carried out the conceptualization, review, and editing.

Sources of Funding for Research Presented in a Scientific Article or Scientific Article Itself

No funding was received for conducting this study.

Conflict of Interest

The author(s) declare no potential conflicts of interest concerning the research, authorship, or publication of this article.

Creative Commons Attribution License 4.0 (Attribution 4.0 International, CC BY 4.0)

This article is published under the terms of the Creative Commons Attribution License 4.0 https://creativecommons.org/licenses/by/4.0/deed.en_US